PRZEGLĄD ELEKTROTECHNICZNY

Ukazuje się od 1919 roku 1b'12

Organ Stowarzyszenia Elektryków Polskich • Wydawnictwo SIGMA-NOT Sp. z o.o.

Hengyu LI, Jun LUO, Jinbo CHEN, Zhixiang LIU ,Shaorong XIE

Shanghai University

Development of Robot Bionic Eye with Spherical Parallel Manipulator Based on Oculomotor Control Model

Abstract. *Vision System is important for autonomous robot. In this paper, a robot bionic vision system, which has the function of the human eye movements, is developed to solve the problem of vision instability during robot working. Firstly, according to the eyeball structure and eye movement characteristics, the mechanism of the bionic eye with three degree of freedom (DOF) is designed by using a spherical parallel manipulator. Because it will be applied in a rough environment, natural frequency of vibration and the maximum deformation of the bionic eye mechanism is gained based on finite-element method(FEM). Then, the control system of the bionic vision is established based on a oculomotor control model, which can compensate the visual error caused by the dynamic changes of the robot attitude and tracking target position. In addition, a bionic vision embedded system with a standard video data interface is developed. Finally, some simulation and physical robot experiments are conducted in harsh environments, and the test results confirm the effectiveness of this bionic vision system. It is also shown that the controller based on oculomotor control model is robust even with external disturbance.*

Streszczenie. *Przedstawiono bioniczny system spełniający funkcję ludzkiego oka. Sztuczne oko porusza się w przestrzeni trójwymiarowej w uwzględnieniem możliwych wibracji. System sterowania może kompensować błędy wynikające z ruchu robota. Przedstqwiono wyniki eksperymentalnego badania w trudnych warunkach pracy. (**Sztuczne oko z równoległym sferycznym manipulatorem bazującym na mechniazmie typu oculomotor**).*

Keywords: Bionic Eye; Robot Vision System; Oculomotor Control Model; Spherical Parallel Manipulator
Słowa kluczowe: sztuczne oko, robot, manipulator..

Introduction

More than 80% of information perception of a human is acquired by the eyes. Correspondingly, vision is very important for autonomous robots[1-2]. There robots are all faced with the problem of disturbances with respect to their vision system during moving and operation process. Systems where a camera is fixed on the robot body or head, without any supplementary stabilization, which provide only poor subjective image quality and resoluti-on[3-4]. Thus, gaze stabilization has been a topic of research in the robotics community by many researchers for a number of years.

Max Meng et al. designed an artificial eye implant, which can detect natural eye movement and the artificial eye to follow the natural eye movement, but is limited to 1-DOF [5]. T. B. Wolfe et al. constructed a 2-DOF eye prosthesis, due to the used shape-memory alloy actuators, and only small velocities can be achieved[6]. Two axes of camera frame could provide images that can be digitalized and vision processed to compensate for distortions. However, the torsion axis is crucial for realizing accurate human eye captured images with a proper sampling[7]. As a result, 3-DOF robot vision devices are recently becoming a focus of research. Wang X. Y. et al. proposed a novel humanoid robot eye, which is driven by six Pneumatic Artificial Muscles and rotates with 3-DOF[1], but the robot eye requires compressed air. An agile eye was developed by Gosselin and his colleagues, which used six sets of links. The agile eye can also be adapted to robotic vision system, however, the link mechanism surrounds the end effectors and suggests some difficulty encasing the device behind a layer of a humanoid face[7-8]. To overcome this drawback, Y. B. Bang et al. present a 3-DOF anthropo- morphic oculomotor system that reproduces realistic human eye movements for human-sized humanoid applications[9]. Unlike the agile eye, the anthropo-morphic oculomotor simulator was built with bent link segments, whose design maintain motion path behind the eyeball.

Robot eyes described above which have mainly focused on mechanical structure of the eye, but these early robot eyes paid little or no attention to oculomotor neural control model. Classical oculomotor theroy has inspired numerous mathematical models. With the developing of oculomotor anatomy and physiology, not only are there many studies on behavioral, but also the neurophysiology and anatomy of the ocular motor system are well documented. This knowledge makes the ocular motor system a perfect candidate for modeling. Shibata et al. not only trickle the problem of gaze stabilization but also emphasize the problem of the dynamic nature of the oculomotor system[10-11]. A. Lenz et al. studied robot eye equipment system that actuated by motor and pneumatic artificial muscles, respectively[3-4]. They presented a model of vestibulo-ocular reflex (VOR) based on cerebellar function, and the model is implemented and evaluated in the control of the robot eye. We are engaged in studying bionic eye at present [12-13], and our goal is to develop a robot bionic vision system that is similar in some function of human eye.

The rest of the paper is organized as follows. In Section 2, according to the eye movement characteristics, we present the Mechanism design of the bionic eye. Section 3 presents the oculomotor control system and attitude calculation of Inverse Kinematics. Section 4 gives the results of the bionic eye, and the results shows the effectiveness of proposed system. Finally, a brief summary are discussed in Section 5.

Mechanism Design of Bioinic Eye

Structure and movement characteristics of eye

The eyes are rotated by the synergistic action of three pairs of three pairs of extraocular muscles, as shown in Figure 1. The eye can rotate from side to side around the x-axis. Rotate around the horizontal y-axis leads to eye movements that are directed upward or downward. Torsional eye movement occurs around the z-axis[5]. The horizontal components of eye rotations are generated by the medial rectus (mr) and lateral rectus (lr) muscles. Vertical and torsional movements are accomplished by the activation of combinations of the superior/inferior rectus (sr/ir) and superior/inferior oblique (so/io) pairs.

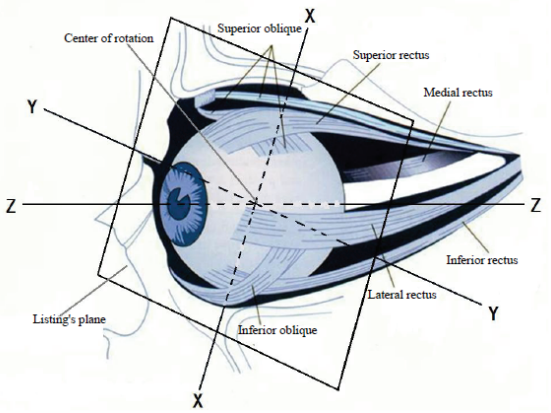

Fig. 1.Structure diagram of extraocular muscles

Eye movements are stereotyped and obey certain 'laws'. Listing's law is a term used to describe the three-dimensional orientation of the eye and its axes of rotation. The expression of Listing's law can be simplified by creating a coordinate system where the origin is primary position, the vertical and horizontal axes of rotation are aligned in Listing's plane, and the torsional axis is orthogonal to Listing's plane (Fig.1). In this coordinate system, Listing's law simply states that torsional component of eye orientation is held at zero. Ignoring the small of translations that occur during ocular rotations, the eye can be modeled as a ball-and-socket joint with a fixed centre of rotation and three rotational degrees of freedom.

Mechanism Design

Parallel manipulators with reduced DOF have received much attention from many researchers recently due to their lower cost, high precision and flexibility[7-9,14]. Spherical parallel manipulator (SPM) can be used for generating 3-axis rotational motions. One of the most distinct features of the human vision system is that it provides smooth and fast 3-DOF rotations in very compact system. Because the SPMs just has these characteristics, the it is adopted as the eyeball mechanism.

The architecture of the spherical parallel manipulator under consideration is shown in Figure 2 [12]. It consists of a upper layer and a base which are connected by three pairs of identical kinematic subchains. In each chin, there is one fixed revolute joint Z_i and two free revolute joints X_i and Y_i connecting the proximal link to the distal link and the distal link to the upper layer, respectively. The axes of all revolute joints intersect at a common point 0 which is referred to as the rotational center. The actuated angle θ_i can be individually manipulated by a servo motor, thereby providing the upper layer with a up to 3-axis rotational capability[14].

The kinematic design of the spherical parallel manipulator is basically an issue of how to determine α_1, α_2, β_1, β_2, and η. Dexterity is the most significant factors dominating the kinematic performance of the manipulators. We presented a method to determine structure parameters of SPM based on the required workspace of the bionic eye and the special of its configuration, which utilizes the worst-case performance index as the optimizing target in required workspace. The optimizing process is carried out in required workspace instead of reachable workspace. It not only reduces the complexity calculation of reachable workspace, but also improves the optimal performance of the eye workspace [12]. Finally, the SPM's parameters are gained by this model and shown as follow: α_1 =60°, α_2 =60°, β_1 =30°, β_2 = 130° and η =127°. The mechanism diagram of the bionic eye is presented as Figure 3. Its main parts are as follows: 1-high-speed camera; 2-camera bracket;3-upper platform; 4-attitude sensors; 5-upper link; 6-lower link; 7-motor protection equipment; 8-Fixed gasket; 9-Electrical installations; 10-base. The actuators are located on the base of the mechanism and consist of maxon E C motors (EC45, Disc motor, Φ45mm, 30watt) and mini- gearheads. The mini-gearheads can provide high position accuracy and smoothness of operation in a very compact package.

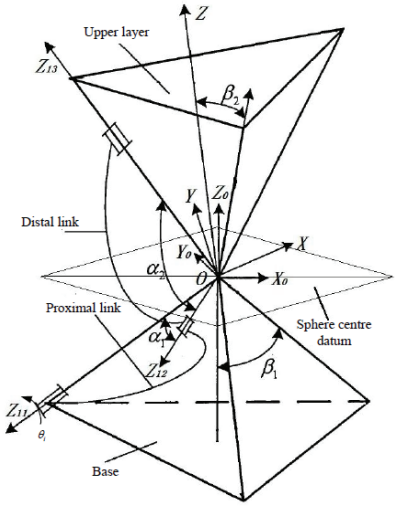

Fig. 2. Kinematic sketch of a spherical parallel manipulator

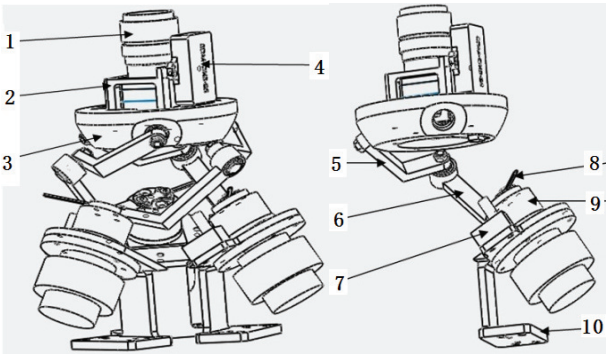

Fig. 3. Mechanism diagram of the bionic eye

As the robot bionic eye is used in a rough environment, it is important to conduct modal analysis for the mechanical structure of bionic eye. Modal analysis is a technology that is used to ascertain the natural frequencies and vibration mold-state parameters of the structure. The finite element analysis (FEA) method was utilized to analyze the mechanical modal of the bionic eye. For an n-DOF system, its general dynamics equation is shown in (1):

$$[M]\{\ddot{u}\}+[C]\{\dot{u}\}+[K]\{u\}=\{F(t)\} \quad (1)$$

For modal analysis, then F(t) =0, [C] is ignored usually. and for harmonic response analysis, F(t) and $u(t)$ are assumed to be harmonic function, for example: $Xsin(\omega t)$, where X is amplitude, ω is frequency, and its unit is rad/s. As for the bionic eye we designed, we assume it is free vibration and ignore damping influence. So the equation is:

$$[M]\{\ddot{U}(t)\}+[K]\{U(t)\}=0 \tag{2}$$

If it is harmonic vibration, it is u = Usin(ωt), the equation is:

$$([K]-\omega_i^2[M])\{\phi_i\}=0 \tag{3}$$

So as for the model analysis of structure, its circular frequency ω_i and mode of vibration ϕ_i can be obtained from the aforementioned equation, whose equation root (also called eigen value) is ω_1^2, the corresponding vector $\{u\}_i$ is called eigen vector, where i varied from 1 to the number of DOF. Square root of eigen value is ω_i, which is natural circular frequency whose unit is rad/s, then we can get natural frequency by the formula $f_i = \omega_i/2\pi$ (rad/s). Eigen vector shows the mode shape which is the shape of structure working with the frequency f_i. Figure 4 and figure 5 are the meshing diagram of the bionic eye mechanism and the 1th shock-type of the mechanism, respectively.

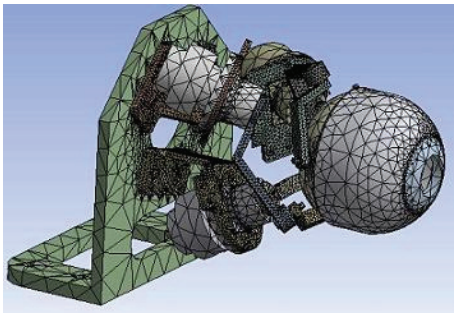

Fig. 4. The meshing of the bionic eye mechanism

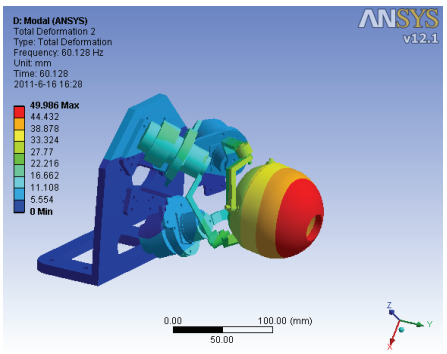

Fig. 5. The first shock-type of the bionic eye mechanism

Table 1. The Max-deformation and Natural frequency of the bionic eye mechanism

Mode order N	Natural frequency /Hz	Max-deformation /mm
1	60.128	49.986
2	67.007	53.761
3	109.29	43.455
4	126.06	36.973
5	199.11	41.101
6	224.96	61.688

As shown in table 1, resonance will occur when the bionic eye is working with one of six natural frequency and the bionic eye will deform a lot. So natural frequency must be avoided during the bionic eye working. In addition, table 1 also shows that the most fragile part is the motor bracket and base. so the thickness of the motor brackets are increased and a rig is designed to strengthen the base. The bionic eye of SPM is shown in Figure 6.

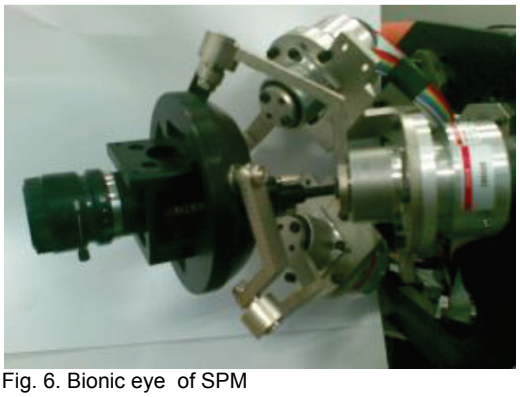

Fig. 6. Bionic eye of SPM

Oculomotor control system

Oculomotor neural paths

Figure.7 shows the oculomotor neural paths based on the previous study, which is regard as a control system, eyeball and ocular muscles are the controlled objects. The neural pathway starting from the retina via optic chiasm merges with the pathway from the retina of another eye, and then pursues two different routes[13,15-16]. First pathway: lateral geniculate nucleus(LGN)→visual cortex (VC) → dorsolateral pontine nucleus (DLPN) →vestibular nucleus (VN). Second route: the nucleus of the tract (NOT) → nucleus reticularis tegmenti pontis (NRTP) → VN. Besides the signal from the retina, the vestibule nucleus accepts the saccadic signal from superior colliculus and the head rotational signal detected by vestibular receptors. The oculomotor control loop stating from the VN: VN → oculomotor nucleus (OMN)→Medial rectus (MR) or VN→ abducens nucle(AN)→lateral rectus (LR). Figure 7 provides a simplified diagram of some the feed-forward connections essential for eye movements. All of these cortical areas have direct projections to brainstem areas including rostral nucleus reticularis tegmenti pontis (rNRTP). These brainstem areas canters project to different regions of the cerebellum (e.g. flocculus), which play complementary roles in eye movements. The input signals are transferred through mossy fibers (mf). The signals coming from NRTP are retinal slip signals and retinal slip velocity signals [17,18].

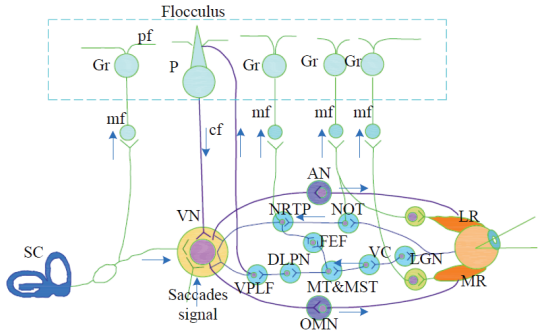

Fig. 7. Oculomotor neural paths.

Oculomotor control modeling

The vestibulo-ocular reflex (VOR) is ultimately driven by signals from the vestibular apparatus in the inner ear. Very early in the history of neuroscience the VOR is regarded as

a simple neural system mediated by a three-neuron arc and displaying a distinct function[18-19]. The semicircular canals code the attitude information of head rotation, and the information is passed on to interneuron in vestibular nuclei in the brainstem. From here the signal, after some integration, is further relayed on to the motor neurons which induce muscle contraction. Smooth pursuit eye movements allow the eyes to closely follow a moving object. Pursuit differs from the VOR, which only occurs during movements of the head and serves to stabilize gaze on a stationary object. The smooth pursuit is modified by ongoing visual feedback. The neural circuitry underlying smooth pursuit is an object of debate. The first step towards the initiation of pursuit is to see a moving target. Signals from the retina ascend through the lateral geniculate nucleus and activate neurons in primary visual cortex. Primary visual cortex sends the information about the target to the middle temporal visual cortex, which responds very selectively to directions of movement. The processing of motion in this area is necessary for smooth pursuit responses. This sensory area provides the motion signal, which may or may not be smoothly pursued.

Without taking into account non-linearities or adaptation effects, the dynamics of the semicircular canals can be regarded as a first-order linear filter $C(s)$. The eye plant is responsible for converting motor neural signals into eye movement, and the horizontal eye plant can be modeled as $P(s)$. The brainstem is modeled as a first-order leaky integrator plus a pure dc gain[3], and the laplace transform of the brainstem model is $NI(s)$. Flocculus plays an import role in eye movement. We used high-precision repeat-error-compensation controller to imitate the Flocculus, it is to be expected that the role of repetitive control gain declined in the high frequency range, a low pass filter $Q(s)$ is added in the repetitive control. Transfer function of these nervous organs' model is shown in equation (4). Block diagram for the control system of the VOR is shown in Figure.8.

$$\begin{cases} C(s)=\dfrac{T_c}{sT_c+1} \\ P(s)=\dfrac{1}{sT_e+1} \\ NI(s)=\dfrac{T_n}{sT_n+1}+g_e \\ Q(s)=\dfrac{e^{-ls}}{sT_q+1} \end{cases} \tag{4}$$

$$E(s)=H(s)\frac{-\alpha T_v T_n s^2}{(sT_v+1)(sT_n+1)}+\varepsilon(s)[(\lambda s+\gamma)+\frac{(k+\mu s)e^{-ls}}{sT_q+1}]\left(g_e+\frac{T_n}{sT_n+1}\right)\frac{1}{sT_e+1} \tag{5}$$

The mathematical control model can be obtained from Figure 8, which can be stated as equation (5). H(s) is head angular input, $E(s)$ is the eye position output, ε(s) represents the error of retinal slip displacement, and $\varepsilon(s)=T(s)-H(s)-E(s)$. Where T_v=16s, T_e= 0.24s, T_n = 25, g_e = 0.24, T_q =0.2, T_e =0.24s, α =1, λ =1, γ =1, κ =2.5, l =0.012s.

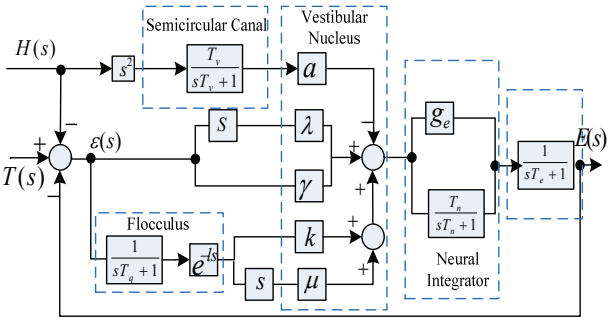

Fig. 8. Block diagram for the oculomotor control system

Power Broken Phase Protection Circuit

As shown in figure 2, a fixed coordinate system $0-X_0Y_0Z_0$ with sphere center 0 as the origin, Moving coordinate system $0-XYZ$ and coupling coordiante system $0-X_{ij}Y_{ij}Z_{ij}$ (i, j =1,2,3) are built [12,14]. Z_0 is the connection of the based center H and the origin 0, whose positive direction points at the upper platform. Z axis is the connection of 0 and the upper platform center, whose positive direction points at the upper platform. Z_{ij} axis is the direction of the j-th revolute of the i-th branch, whose positive direction points outside the ball. X_0 axis is the normal direction of the plane formed by Z_0 and Z_{11}. X axis is the normal direction of the plane formed by Z_0 and Z_{13}. X_{ij} axis is the normal direction of the plane formed by Z_{ij} and X_{ij+1}. Y axis direction is determined by the right-hand rule. To the base, the eye movements are only roation movements are only rotation movements. The eye attitude can be expressed by direction cosine matrix R_{XYZ} of moving coordinate system $0-XYZ$ to fixed coordinate system $0-XYZ$.

$$\boldsymbol{R}_{XYZ}=\begin{bmatrix} c\phi_Y c\phi_Z & s\phi_X s\phi_Y c\phi_Z-c\phi_X s\phi_Z & c\phi_X s\phi_Y c\phi_Z+s\phi_X s\phi_Z \\ c\phi_Y s\phi_Z & s\phi_X s\phi_Y s\phi_Z+c\phi_X c\phi_Z & c\phi_X s\phi_Y s\phi_Z-c\phi_X c\phi_Z \\ -s\phi_Y & s\phi_X c\phi_Y & c\phi_X c\phi_Z \end{bmatrix} \tag{6}$$

where ϕ_X, ϕ_Y, ϕ_Z, respectively represents pan, tilt, and pin a ngles, $s\phi_X$, $c\phi_X$ respectively means $sin\phi_X$ and $cos\phi_X$.

Vector definition: u_i along Z_i, v_i along Z_{i2}, w_i along Z_{13}. Direction vectors of u_i, v_i can be figured out in fixed coordinate system $0-X_0Y_0Z_0$ by attitude transformation.

$$u_i=\begin{bmatrix} \frac{1}{2}s\eta_{1i} & -\frac{1}{2}c\eta_{1i} & -\frac{\sqrt{3}}{2} \end{bmatrix}^T \tag{7}$$

$$v_i=\begin{bmatrix} \frac{\sqrt{3}}{2}c\eta_{1i}s\theta_i-\frac{3}{4}s\eta_{1i}c\theta_i+\frac{1}{4}s\eta_{1i} \\ \frac{\sqrt{3}}{2}s\eta_{1i}s\theta_i+\frac{3}{4}c\eta_{1i}c\theta_i-\frac{1}{4}c\eta_{1i} \\ -\frac{\sqrt{3}}{4}c\theta_i-\frac{\sqrt{3}}{4} \end{bmatrix} \tag{8}$$

$$\boldsymbol{w}_i = \begin{bmatrix} \mathrm{s}130^\circ \mathrm{s}\eta_{2i} \mathrm{c}\phi_Y \mathrm{c}\phi_Z + \mathrm{s}130^\circ \mathrm{c}\eta_{2i} \mathrm{c}\phi_X \mathrm{s}\phi_Z - \mathrm{s}130^\circ \mathrm{c}\eta_{2i} \mathrm{s}\phi_X \mathrm{s}\phi_Y \mathrm{c}\phi_Z + \mathrm{c}130^\circ \mathrm{s}\phi_X \mathrm{s}\phi_Z + \mathrm{c}130^\circ \mathrm{c}\phi_X \mathrm{s}\phi_Y \mathrm{c}\phi_Z \\ \mathrm{s}130^\circ \mathrm{s}\eta_{2i} \mathrm{c}\phi_Y \mathrm{s}\phi_Z - \mathrm{s}130^\circ \mathrm{c}\eta_{2i} \mathrm{c}\phi_X \mathrm{c}\phi_Z - \mathrm{s}130^\circ \mathrm{c}\eta_{2i} \mathrm{s}\phi_X \mathrm{s}\phi_Y \mathrm{c}\phi_Z - \mathrm{c}130^\circ \mathrm{s}\phi_X \mathrm{c}\phi_Z + \mathrm{c}130^\circ \mathrm{c}\phi_X \mathrm{s}\phi_Y \mathrm{s}\phi_Z \\ -\mathrm{s}130^\circ \mathrm{s}\eta_{2i} \mathrm{s}\phi_Y - \mathrm{s}130^\circ \mathrm{c}\eta_{2i} \mathrm{s}\phi_X \mathrm{c}\phi_Y + \mathrm{c}130^\circ \mathrm{c}\phi_X \mathrm{c}\phi_Y \end{bmatrix} \tag{9}$$

The constraint equations are established by using the angle of vector v_i and w_i:

$$v_i^T . w_i = 0.5 \qquad (i = 1,2,3) \tag{10}$$

sorted:

$$A_i \sin\theta_i + B_i \cos\theta_i + C_i = 0 \tag{11}$$

Result of equations:

$$\theta_i = 2\arctan\left(\frac{-A_i + \sqrt{A_i^2 + B_i^2 - C_i^2}}{C_i - B_i}\right) \tag{12}$$

or:

$$\theta_i = 2\arctan\left(\frac{A_i + \sqrt{A_i^2 + B_i^2 - C_i^2}}{B_i - C_i}\right) \tag{13}$$

where A_i, B_i, C_i, is figured out by ϕ_X, ϕ_Y, ϕ_Z, according to assembling from shown in figure 12, formula (13) is inverse kinematics of bionic eyes, to simplify expression, it can be expressed as below:

$$\theta_i = f_{Ri}(\phi_X, \phi_Y, \phi_Z) \tag{14}$$

Experiment and analysis

Oculomotor model simulation

In order to study the model's performance, some simulation experiments were carried on. Simulations were performed using SIMULINK, a graphical interface to MATLAB.

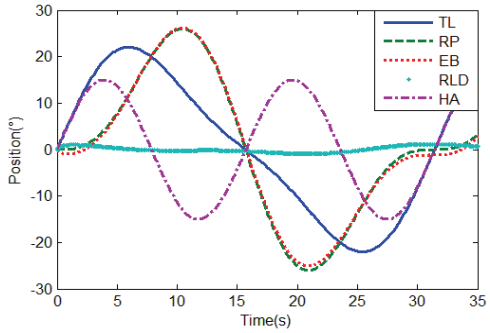

Fig. 9. Simulation results of the compound eye movements under ideal environment.

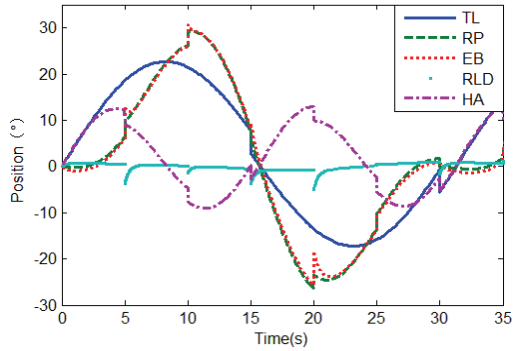

Fig. 10.Simulation results of the compound eye movements during both head attitude and tracking target mutation.

Eye movement is the voluntary or involuntary movement of the eyes, helping in acquiring, fixating and tracking visual stimuli. In fact, because the head and tracking target are in motion, in most instances the human eye's movement is a complex movement that includes smooth pursuit and VOR, etc. The mathematical equations of the compound eye movements can be expressed as equation 5, and the simulation results are shown as Figure. (9-10). HA and EB respectively represent the head attitudes' changes input and the eye ball attitudes' output; TL represents the tracking target location change; RLD represents sliding displacement of the retina; RP represents relative potentiometer between the eyeball and the tracking target location. Figure.9 is the simulation result that robot attitude and tracking target have taken place in sine rule changes, and it indicates that the model can be compensated the errors caused by changes of the robot attitude and tracking target location. Figure 10 is the simulation results that represent both robot posture and tracking target occurring interference during robot target tracking. These simulation results indicate that the model has robust and high accuracy.

Experimental Validations t

In order to study the bionic eye model's performance, an experimental platform based on a tracked robot under harsh environment is designed, and it is shown in Figure 11. The experimental system is different from the previous one in hardware and software systems, which includes a bionic vision system and a traditional vision system. The traditional one is based on PID controller.

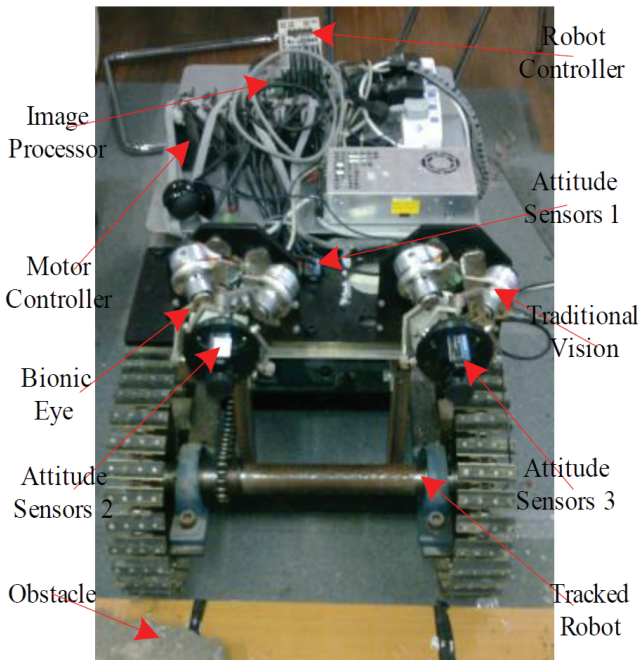

Fig. 11. Experimental platform based on tracked robot

Sensor system is the perception system of the whole bionic vision system. There are two sensor subsystems to get information in the system. One is used to get robot and eyeball attitude information, and the other is used to get

target information by visual sensors. Both they are similar to the vestibular system of the human eye.

To measure angular velocities in three axes, we employ the attitude sensor (3DM-GX-25TM). The device offers a range of output data quantities from fully calibrated inertial measurements (acceleration, angular rate, deltaAngle and deltaVelocity vectors) to computed orientation estimates, including pitch, roll and heading (yaw) or rotation matrix. All quantities are fully temperature compensated and are mathematically aligned to an orthogonal coordinate system. There are three attitude sensors in the experimental system, the sensor 1 measures the attitude changes of the bionic eye, the sensor 2 is used to measure the attitude changes of the tracked robot, and the attitude changes of the traditional vision system are measured by the sensor 3. Thus, the system is similar to the semicircular canal of the human eye. In addition, the image information is gained by using a high-speed camera (Guppy F-033C). The camera is an ultra-compact, inexpensive VGA machine vision camera with CCD sensor (Sony ICX424). At a full resolution, it runs up to 58fps.

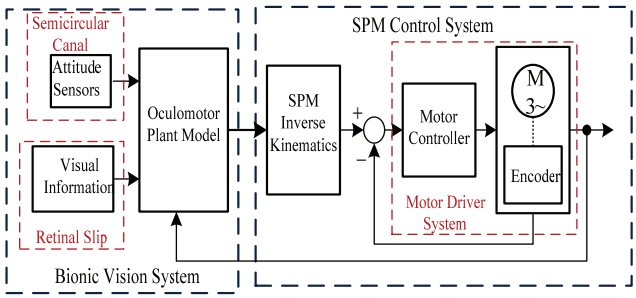

Fig. 12. Control architecture of the bionic eye system

Because the SPM's drive system only utilized steering gear in previous study[12-13], there is a big error in the system. In order to improve the accuracy, a high-precision combination drive system is employed. Figure 12 is the control architecture of the bionic eye system. It is an intelligent closed-loop drive system, which includes EC motor, miniaturized positioning controller, encoder, brake and harmonic reducer. After attitude and visual information obtained and processed by the bionic vision controller, the target position of the upper platform will be gotten. Then motor motion position will be figured out by inverse kinematics algorithm, and path planning and control for drive system will be realized by CANopen protocol.

Aforementioned sensors, actuators, image processing and digital communication device have different signals and interfaces. High real-time performance is required in the bionic vision system. Consequently, it's important to choose the fittest processor in the onboard system. We opted for a MCU TMS320F2812 , featured in high speed and integrated with all the necessary communication ports. The whole experimental system architecture is sketched in figure 13, where the various formats of information exchanges between the instruments are shown. PC platform gets the image information of high-speed cameras by 1394 card and processes images by C# and openCV libraries, thus realizing tracking of targets and getting position pixel information of tracking targets and transmitting it to DSP. Besides, in order to make it convenient to observe and to obtain experiment data, the position and attitude information of the robot and is sent PC platform.

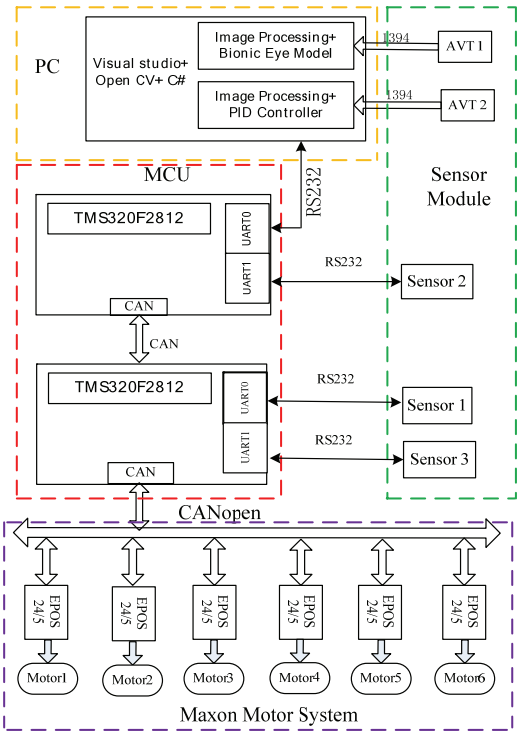

Fig. 13. Whole experimental system architecture

In order to verify the performance of the bionic vision system, some comparison tests between using the bionic model and without using the model are conducted. Figure 14 is the test results using traditional PID controller, and Figure 15 is the test results with using the bionic vision system. RPA and RRA respectively represent the robot attitude in the pitch and roll direction; EPA and ERA respectively represent the eyeball output attitude in the pitch and roll direction. The test results confirm the effectiveness of this bionic vision system. Compared with the conventional PID methods, the bionic vision system is more effective.

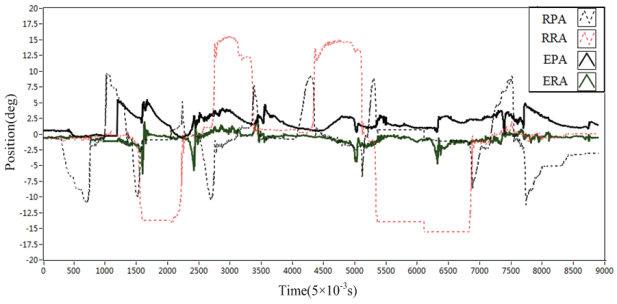

Fig. 14 Experimental results without using control system of the bionic vision

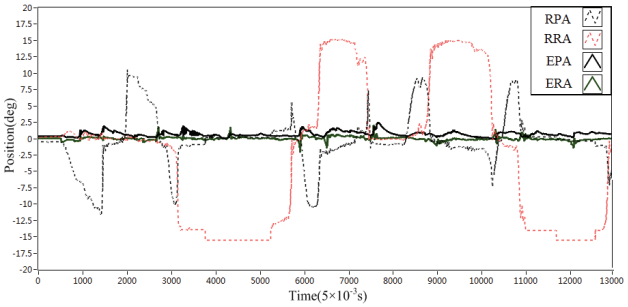

Fig. 15 . Experimental results of with using the PID control system

Conclusions

The human vision system orients each eye with 3-DOF in the directions of horizontal, vertical and torsional axes. in order to accurately replicate the human vision system, the robot bionic eye constructed by the spherical parallel manipulator with 3-DOF is designed based on the characteristics of the human being's eye. ANSYS is utilized to conduct modal and mechanics property analysis respectively. The control system of the bionic eye is based on a oculomotor control model. The model simulation experiments are performed in different environments, and the results show that the model can compensate the visual error caused by the dynamic changes of the robot attitude and target position. Finally, some physical robot experiments are conducted, which also demonstrates the validity and accuracy of the bionic eye. Compared with the conventional PID methods, the bionic vision system is effective.

Acknowledgment

This work was supported by the National Science Foundation of China (No.60975068, 50975168), the Specialized Research fund for the Doctoral Program of Higher Education (No. 20093108110007), "Shu-guang" Project supported by shanghai Municipal Education Commission and shanghai Education Development Foundation (No.09SG37), and the Graduate Innovation Fund of Shanghai University (No. SHUCX111005). The authors also gratefully acknowledge the helpful comments and suggestions of the reviewers, which have improved the presentation.

REFERENCES

[1] X. Y. Wang, Y. Zhang, X. J. Fu, G. S. Xiang, “Design and Kinematic Analysis of a Novel Humanoid Robot Eye Using Pneumatic Artificial Muscles”, Journal of Bionic Engineering, Vol.5, No.3,pp264-270, 2008.

[2] T. Villgrattner, H. Ulbrich, “Design and Control of a Compact High-Dynamic Camera-Orientatation System”, IEEE/ASME Transactions on Mechatronics, vol.16, No.2, pp221-231, 2011.

[3] A Lenz, T. Balakrishnan, A. G. Pipe and C. Melhuish, “An adaptive gaze stabilization controller inspired by the vestibulo-ocular reflex”, Bioinspiration & Biomimetics, vol.3, No.035001, pp1-11,June 2008.

[4] A Lenz, S. R. Anderson, A. G. Pipe, C. Melhuish, P. Dean, and J. Porrill, “Cerebellar-Inspired Adaptive Control of a Robot Eye Actuated by Pneumatic Artificial Muscles”, IEEE Transactions on systems, Man, and Cybernetics-part B: Cybernetics, vol.39, No.6, pp1420-1432, December 2009.

[5] J. Gu, M. Meng, A. Cook, M. G. Faulkner, “A study on natural movement of artificial eye implant”, Robotics and Autonomous Systems, vol.32, No.2, pp153-161(9), August 2000.

[6] T. B. Wolfe, M. G. Faulkner and J. Wolfaardt, “Development of a shape memeory alloy actuator for a robotic eye prosthesis”, Smart Materials and Structures, Vol.14, No.4, pp 759-768, 2005.

[7] C. M. Gosselin, E. St-Pierre, M. Gagne, “On the development of the agile eye”, IEEE Robotics & Automation Magazine, Vol.3, No.4,pp29-37,1996.

[8] C. M. Gosselin, E. St-Pierre, “Development and experimentation of a fast 3-DOF camera-orienting device”, International Journal of Robotics Research, Vol.16, No.5,pp619-630,1997.

[9] Y. B. Bang, J. K. Paik, B. H. Shin, and C. Lee, Luck, “A Three-Degree-of - Freedom Anthropomorphic Oculomotor Simulator”, International Journal of Control, Automation, and Systems, vol.4, No.2, pp227-235, April 2006.

[10] T. Shibata, S. Schaal, “Biomimetic gaze stabilization based on feedback-error-learning with nonparametric regression networks”, Neural Networks, Vol.14, No.2, pp 201-216, 2001.

[11] T. Shibata, H. Tabata, S. Schaal, et al. “A model of smooth pursuit in primates based on learning the target dynamics”, Neural Networks, No.18, 2005, pp213-224.

[12] C. Li, S.R. Xie, H.Y. Li, D. Wang, J. Luo, “Design of Bionic Eye Based on Spherical Parallel Mechanism with Optimized Parameters ”, Robot, vol.32, No.6, pp781-786, Nov 2010.

[13] H.Y. Li, J. Lou, C. Li, L. Li, S.R. Xie, “Active Compensation Method of Robot Visual Error Based on Vestibulo-ocular Reflex ”, Robot, vol.33, No.2, pp197-203, 2011.

[14] T. Huang, X. J. Zeng, Z. P. Zeng, “Dimensional synthesis of spherical parallel manipulators”, Progress in Natural Science, Vol.11,No.1, pp50-57, January 2001.

[15] D. A. Robinson, J. L. Gordon, and S. E. Gordon. “A model of the smooth pursuit eye movement system”, Biol. Cybern. No.55,1986, pp43-57.

[16] D. C. Deno, E. L. Keller, W. F. Crandall. “Dynamical neural network organization of the visual pursuit system”, IEEE Transactions on Biomedical Engineering, Vol.36, No. 1, 1989, pp85-92.

[17] M. Ito. “Cerebellar circuitry as a neuronal machine”, Progress in Neurobiology, No.78, 2006, pp272-303.

[18] X.L. Zhang, H. Wakamatsu. “A unified adaptive oculomotor control model”, International Journal of Adaptive Control and Signal Processing, Vol.15, No.7, 2001, pp697-713.

[19] S. Glasauer. “Current models of the ocular motor system”, Neuro-Opthalmology, No.40, 2007, pp158-174.

***Authors**: prof. dr Hengyu Li, School of Mechatronics Engineering and Automation, Shanghai University, Shanghai, China, and Shanghai Key Laboratory of Mechanical Automation and Robotics, Shanghai, China, E-mail: lihengyub@shu.edu.cn; dr Jun Luo, School of Mechatronics Engineering and Automation, Shanghai University, Shanghai, China, and Shanghai Key Laboratory of Mechanical Automation and Robotics, Shanghai, China.*